Acta Cryst. (1975). B31, 1041

Crystal Structures of Pyroxene-Type $ZnSiO_3$ and $ZnMgSi_2O_6$

BY N. MORIMOTO AND Y. NAKAJIMA

Institute of Scientific and Industrial Research, Osaka University, Suita 565, *Japan*

Y. SYONO

Institute for Iron, Steel, and Other Metals, Tohoku University, Sendai 980, *Japan*

S. AKIMOTO

Institute for Solid State Physics, University of Tokyo, Roppongi, Minato-ku, Tokyo 106, *Japan*

AND Y. MATSUI

Institute for Thermal Spring Research, Okayama University, Misasa, Tottori-Ken 68202, *Japan*

(*Received* 24 *June* 1974; *accepted* 20 *November* 1974)

The crystal structures of two pyroxene polymorphs of $ZnSiO_3$ and the orthopyroxene of $ZnMgSi_2O_6$ have been studied. The monoclinic $ZnSiO_3$ crystallizes in the space group $C2/c$ with $a=9{\cdot}787$, $b=9{\cdot}161$, $c=5{\cdot}296$ Å, $\beta=111{\cdot}42°$, $Z=8$; orthorhombic $ZnSiO_3$, *Pbca*, $a=18{\cdot}204$, $b=9{\cdot}087$, $c=5{\cdot}278$ Å, $Z=16$ and orthorhombic $ZnMgSi_2O_6$, $a=18{\cdot}201$, $b=8{\cdot}916$, $c=5{\cdot}209$ Å, $Z=16$. In the structure of the monoclinic $ZnSiO_3$, Zn atoms are coordinated octahedrally (at M1 sites) and tetrahedrally (at M2 sites). The Zn atoms at the M2 sites are not coordinated by the bridging oxygen [O(3)] of the SiO_3 chains. In the orthorhombic $ZnSiO_3$, however, Zn atoms at the M2 sites have an irregular octahedral coordination including O(3) atoms. Because of the difference in coordination of O(3) to Zn atoms, the shape of the SiO_3 chains in the two polymorphs of $ZnSiO_3$ is different. The structure of the orthorhombic $ZnMgSi_2O_6$ is intermediate between that of enstatite ($MgSiO_3$) and the orthorhombic $ZnSiO_3$. Zn atoms are partially ordered in M1 and M2 sites with site occupancies of 36 and 64% respectively.

Introduction

Most of the common monoclinic pyroxenes are divided into two groups, the pyroxenes in space group $C2/c$ and those in $P2_1/c$. In general, the pyroxenes in $P2_1/c$ have β angles greater than 108·0°, which are larger than those of the pyroxenes in $C2/c$ (Table 1). The existence of polymorphic relations in pyroxenes between the orthorhombic form in *Pbca* and the monoclinic in $P2_1/c$ is known. No monoclinic pyroxene in $C2/c$ has ever been reported to have orthorhombic polymorphs.

Two polymorphs of $ZnSiO_3$ have been synthesized under high pressures and temperatures by Syono, Akimoto & Matsui (1971). They have the monoclinic ($C2/c$) and orthorhombic (*Pbca*) pyroxene structures. According to Syono *et al.* (1971), the monoclinic $ZnSiO_3$ (hereinafter $ZnSiO_3(M)$) is stable above 30kb and 850°C, while the orthorhombic $ZnSiO_3$ ($ZnSiO_3(O)$) is metastable at all conditions. $ZnSiO_3(M)$ has been found to have the largest β angle in the clinopyroxenes, which is comparable with that of spodumene in $C2$, in spite of its space group being $C2/c$. Furthermore, this is the first example of a $C2/c$ pyroxene which has a polymorphic form in *Pbca*. These characteristics are considered to be due to the special behaviour of Zn atoms in the structures in which tetrahedral coordination is predominant, such as in willemite (Zn_2SiO_4), Zn_2SiO_4II (Marumo & Syono, 1971), hardystonite ($Ca_2ZnSi_2O_7$) (Louisnathan, 1969), hemimorphite [$Zn_4Si_2O_7(OH)_2H_2O$] (McDonald & Cruickshank, 1967) and hodgkinsonite [$Zn_2Mn(OH)_2SiO_7$] (Rentzeperis, 1963).

In this investigation, the structure determinations of the two polymorphs of $ZnSiO_3$ and the orthorhombic $ZnMgSi_2O_6$, (hereinafter $ZnMgSi_2O_6(O)$), have been carried out in order to elucidate the following points: (*a*) the structural characteristics of $ZnSiO_3(M)$ in which the β angle is exceptionally large in the monoclinic pyroxenes in $C2/c$, (*b*) the structural relation between $ZnSiO_3(M)$ and $ZnSiO_3(O)$ as the first polymorphic relation between the pyroxenes of *Pbca* and $C2/c$, and (*c*) the characteristic ligands of Zn atoms in the pyroxene structures.

Experimental

The cell dimensions, space groups and densities at atmospheric pressure are given for the two polymorphs of $ZnSiO_3$ and orthorhombic $ZnMgSi_2O_6$ in Table 2. The space groups were determined by Weissenberg and precession methods, and cell dimensions calculated from several reflexions measured on an automatic four-circle diffractometer. The three-dimensional intensity data were collected on the diffractometer with Mo $K\alpha$ radiation (Zr-filtered) for the three crystals and the $\omega/2\theta$ scan method. The intensities were corrected for

Lorentz and polarization effects. No absorption correction was made because of the small sizes of the crystal specimens.

FACOM 230–60 at the University of Kyoto and NEAC 700 at Osaka University were used for the computations of the structure determination and the refinements. The latter were carried out by the full-matrix least-squares method with *ORFLS* (Busing, Martin & Levy, 1962), modified by Sakurai (1967), and by Fourier syntheses with the program *RSSFR-5* (Sakurai, 1967) of the UNICS system. Scattering factors and the dispersion corrections with real and imaginary terms for Zn^{2+}, Mg^{2+} and Si^{4+} were taken from *International Tables for X-ray Crystallography* (1962), while scattering factors for O^{2-} were taken from the values reported by Tokonami (1965). Dispersion corrections for O^{2-} were assumed to be zero.

(*a*) $ZnSiO_3(M)$

Data collection: The single crystals of $ZnSiO_3(M)$ were synthesized from mixtures of ZnO and SiO_2 in the required proportions at 1400°C and 70 kbar by the tetrahedral-anvil press. A colourless transparent crystal with prismatic shape elongated along the *c* axis (0·05 × 0·045 × 0·06 mm) was used for collecting intensity data. Of 1101 symmetrically independent reflexions, 52 were less than or equal to the background value and were regarded as having zero intensity.

Structure refinement: Structure refinement was initiated using the atomic coordinates of diopside (Warren & Bragg, 1928) and isotropic temperature factors of 0·5 for Zn and Si atoms and 1·0 for oxygen atoms. The least-squares method was carried out with weights equal to $1/\sigma^2$ where σ represents the estimated standard

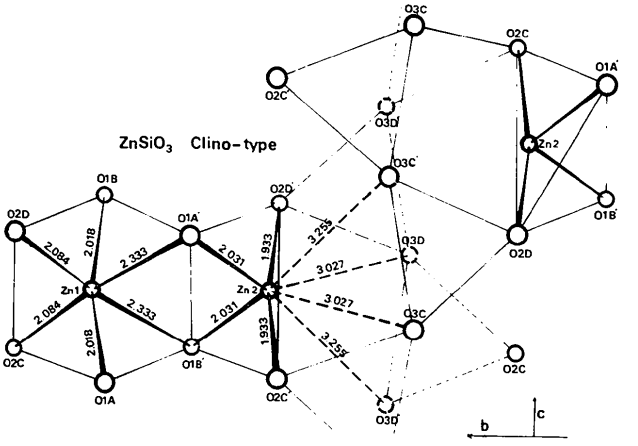

Fig. 1. Part of the structure of $ZnSiO_3$ (*M*) projected on (100) along the *a** axis. Zn(2) shows a characteristic tetrahedral arrangement. O(3) atoms are removed from the coordination. The letters *A*, *B*, *C* and *D* follow the designation of Burnham, Clark, Papike & Prewitt (1967).

Table 1. *Relations between the ionic radii of metals at the* M1 *and* M2 *sites, β angle and space group in some important end-members of clinopyroxenes*

M2 ion	Radius (Å)	M1 ion	Radius (Å)	β(°)	Space group
Ca^{2+} (VIII)	1·12	Mn^{2+}(VI)	0·82	105·48(1)	
		Fe^{2+} (VI)	0·77	104·33(2)	
		Mg^{2+}(VI)	0·72	105·63(3)	
		In^{3+} (VI)	0·79	107·00(4)	*C*2/*c*
Na^{+} (VIII)	1·16	Fe^{3+} (VI)	0·65	107·42(3)	
		Cr^{3+} (VI)	0·62	107·44(3)	
		Al^{3+} (VI)	0·53	107·58(5)	
Mn^{2+}(VI)	0·82	Mn^{2+}(VI)	0·82	108·22(6)	
Fe^{2+} (VI)	0·77	Fe^{2+} (VI)	0·77	108·38(6)	
Co^{2+} (VI)	0·735	Co^{2+} (VI)	0·735	108·45(6)	*P*2$_1$/*c*
Mg^{2+}(VI)	0·72	Mg^{2+}(VI)	0·72	108·33(6)	
Li^{+} (VI)	0·74	Fe^{3+} (VI)	0·65	110·16(3)	
		Al^{3+} (VI)	0·53	110·10(3)	*C*2
Zn^{2+} (IV)	0·60	Zn^{2+} (VI)	0·75	111·42(7)	*C*2/*c*

(1) Freed & Peacor (1967). (2) Deer, Howie & Zussman (1963). (3) Clark *et al.* (1969). (4) Christensen & Hazell (1967). (5) Prewitt & Burnham (1966). (6) Syono *et al.* (1971). (7) Present study.

Table 2. *Crystal data for* $ZnSiO_3(M)$, $ZnSiO_3(O)$ *and* $ZnMgSi_2O_6(O)$ *compared with enstatite* ($MgSiO_3$) (*Morimoto & Koto*, 1969)

	$ZnSiO_3(M)$	$ZnSiO_3(O)$	$ZnMgSi_2O_6(O)$	Enstatite
a (Å)	9·787 (3)	18·204 (5)	18·201 (5)	18·210 (10)
b (Å)	9·161 (2)	9·087 (3)	8·916 (2)	8·812 (05)
c (Å)	5·296 (1)	5·278 (2)	5·209 (2)	5·178 (04)
β (°)	111·42 (3)			
V (Å^3)	442·0 (2)	873·1 (3)	842·2 (3)	830·89
Z	8	16	16	16
Calc. *D* (g cm^{-3})	4·250	4·303	3·800	
Space group	*C*2/*c*	*Pbca*	*Pbca*	*Pbca*

deviation computed from the counting statistics. For a reflexion of zero intensity σ was 5·0. The R value obtained for the initial model was 0·46. The displacement of Zn in the M2 site was found by F_o and $F_o - F_c$ syntheses. Three cycles of least-squares refinement of the atomic coordinates and one scale factor were made, keeping the isotropic temperature factor constant. In the next three cycles, individual isotropic temperature factors were allowed to vary. The residual and weighted residual for all 1101 reflexions were reduced to 0·057 and 0·036 respectively. Finally the isotropic temperature factors were converted to the anisotropic form and after three cycles of refinement, varying the scale factor, atomic coordinates and anisotropic temperature factors, there were no further changes in the parameters. The final residual and weighted residual are 0·046 and 0·031, respectively, for all reflexions. The final parameters, individual anisotropic temperature factors and equivalent isotropic temperature factors are listed with their estimated standard deviations in Table 3.

(*b*) $ZnSiO_3(O)$

Data collection: The metastable single crystals of $ZnSiO_3(O)$ were separated from the quench-products at 1400°C and 84 kbar for Zn_2SiO_4. The run had been carried out using the tetrahedral-anvil press for the purpose of synthesizing single crystals of Zn_2SiO_4III. 2:1 mixtures of ZnO and SiO_2 were used as starting materials. The cell dimensions of $ZnSiO_3(O)$ are compared with those of enstatite in Table 2. The crystal used for the data collection was an approximately rhombohedral prism (0·07 × 0·08 × 0·10 mm). Of the 1263 reflexions observed 118 were less than or equal to the background values and were regarded as having zero intensity.

Structure refinement: The refinement was initiated using Morimoto & Koto's (1969) atomic coordinates and isotropic temperature factors for enstatite. After several cycles of least-squares refinement with the same weighting scheme as for $ZnSiO_3(M)$, during which atomic coordinates, isotropic temperature factors, and one scale factor were varied, the R value of 0·090 and the weighted R value of 0·049 were obtained. Temperature factors were then converted to the anisotropic form and four cycles of refinement with unit weights further reduced the R value for all 1263 reflexions to 0·073. The final atomic parameters, individual anisotropic temperature factors and the equivalent isotropic temperature factors are listed with their estimated standard deviations in Table 4.

(*c*) $ZnMgSi_2O_6(O)$

Data collection: The structure of $ZnMgSi_2O_6(O)$ has been determined from a single crystal synthesized at 1400°C and 70 kbar from a mixture of ZnO, SiO_2 and $MgSiO_3$ glass by the tetrahedral-anvil press. Only a small single crystal (0·04 × 0·04 × 0·05 mm) was available. Of 1296 symmetrically independent reflexions, 361 were less than or equal to the σF values, including 273 reflexions which had zero intensity as a result of the small size of the crystal. These were omitted from the structure refinement.

Structure refinement: The refinement was initiated using the atomic coordinates and isotropic temperature factors of $ZnSiO_3(O)$, assuming that Zn and Mg atoms

Table 3. *Atomic coordinates, anisotropic temperature factors* (× 10⁴) *and equivalent isotropic temperature factors for atoms in* $ZnSiO_3(M)$

Standard deviations are given in parentheses.

	x	y	z	B_{11}	B_{22}	B_{33}	B_{12}	B_{31}	B_{23}	B
Zn(1)	0·5	0·3919 (1)	0·25	22 (1)	22 (1)	40 (2)		5 (1)		0·58 (1)
Zn(2)	0·0	0·2361 (1)	0·25	20 (1)	19 (1)	51 (2)		8 (1)		0·53 (1)
Si	0·3016 (1)	0·0849 (1)	0·2668 (2)	13 (1)	9 (1)	35 (3)	−1 (1)	5 (2)	−2 (2)	0·32 (2)
O(1)	0·1241 (3)	0·0868 (3)	0·1473 (6)	18 (3)	18 (3)	63 (10)	1 (2)	11 (5)	0 (5)	0·61 (5)
O(2)	0·3787 (3)	0·2393 (3)	0·3719 (6)	29 (3)	19 (3)	48 (10)	−4 (2)	15 (5)	−5 (5)	0·71 (5)
O(3)	0·3533 (3)	0·0238 (3)	0·0273 (5)	18 (3)	27 (3)	53 (10)	−7 (2)	9 (5)	−16 (5)	0·67 (5)

Table 4. *Atomic coordinates, anisotropic temperature factors* (× 10⁴) *and equivalent isotropic temperature factors for atoms in* $ZnSiO_3(O)$

Standard deviations are given in parentheses.

	x	y	z	B_{11}	B_{22}	B_{33}	B_{12}	B_{31}	B_{23}	B
Zn(1)	0·1255 (1)	0·3559 (1)	0·4039 (2)	7 (0)	14 (1)	52 (3)	1 (0)	3 (1)	−2 (1)	0·65 (2)
Zn(2)	0·3761 (1)	0·5092 (1)	0·4005 (2)	7 (0)	13 (1)	53 (3)	−1 (0)	−2 (1)	4 (1)	0·64 (2)
Si(*A*)	0·2741 (1)	0·3363 (2)	0·0867 (4)	5 (1)	4 (2)	27 (6)	1 (1)	2 (2)	−1 (3)	0·34 (3)
Si(*B*)	0·4730 (1)	0·1656 (2)	0·2839 (4)	4 (1)	7 (2)	34 (6)	0 (1)	2 (2)	6 (3)	0·38 (3)
O(1*A*)	0·1853 (3)	0·3346 (6)	0·082 (1)	6 (2)	22 (6)	58 (18)	3 (3)	4 (4)	−7 (9)	0·69 (9)
O(2*A*)	0·3115 (3)	0·4966 (6)	0·104 (1)	4 (1)	17 (6)	80 (19)	3 (2)	−4 (4)	2 (9)	0·57 (9)
O(3*A*)	0·3039 (3)	0·2521 (7)	0·340 (1)	6 (1)	36 (6)	63 (18)	4 (3)	6 (5)	21 (10)	0·84 (10)
O(1*B*)	0·5621 (3)	0·3389 (6)	0·780 (1)	8 (2)	18 (6)	73 (19)	0 (2)	3 (5)	12 (9)	0·82 (10)
O(2*B*)	0·4327 (3)	0·4853 (6)	0·704 (1)	8 (2)	10 (5)	17 (16)	4 (2)	0 (4)	−11 (8)	0·53 (9)
O(3*B*)	0·4488 (3)	0·2100 (6)	0·571 (1)	5 (1)	15 (6)	48 (18)	1 (2)	3 (4)	−13 (8)	0·59 (9)

were in complete disorder at the M1 and M2 sites. F_o and $F_o - F_c$ Fourier syntheses were made to determine the site occupancies of Zn and Mg at the two sites. The occupancies obtained are Mg 0·64 and Zn 0·36 for the M1 site and Mg 0·36 and Zn 0·64 for the M2 site. Three cycles of refinement of the atomic coordinates and one scale factor were made keeping the isotropic temperature factors constant. In the next three cycles, individual isotropic temperature factors were allowed to vary. The final R and the weighted R were reduced to 0·101 and 0·049, respectively, for 935 observed reflexions. Conversion of the temperature factors to the anisotropic form, however, did not lead to any improvement in the R values. This is thought to be due to inaccurate measurements of the intensities of relatively weak reflexions as a result of the small size of the crystal. The final atomic coordinates and the individual isotropic temperature factors with their estimated standard deviations are listed in Table 5.†

Table 5. *Atomic coordinates and isotropic temperature factors for atoms in* $ZnMgSi_2O_6(O)$

Standard deviations are given in parentheses.

	x	y	z	B
M1	0·1245 (2)	0·3491 (4)	0·3798 (7)	0·98 (5)
M2	0·3757 (1)	0·4964 (3)	0·3769 (5)	0·71 (3)
Si(A)	0·2731 (2)	0·3397 (5)	0·0652 (7)	0·14 (5)
Si(B)	0·4731 (2)	0·1638 (5)	0·2900 (8)	0·19 (5)
O(1A)	0·1847 (6)	0·338 (1)	0·049 (2)	0·46 (15)
O(2A)	0·3104 (5)	0·504 (1)	0·067 (2)	0·23 (13)
O(3A)	0·3040 (5)	0·267 (1)	0·336 (2)	0·36 (15)
O(1B)	0·5633 (6)	0·337 (1)	0·792 (2)	0·33 (14)
O(2B)	0·4329 (5)	0·482 (2)	0·696 (2)	0·03 (13)
O(3B)	0·4483 (5)	0·202 (1)	0·594 (2)	0·20 (13)

Discussion of the structures

(*a*) $ZnSiO_3(M)$

The refined structure of $ZnSiO_3(M)$ is different from the structures of diopside and other monoclinic pyroxenes in $C2/c$. Selected interatomic distances and angles were computed for $ZnSiO_3(M)$ using the program *RSDA*-4 of the UNICS system (Sakurai, 1967) (Table 6).

A part of the structure of $ZnSiO_3(M)$ is projected on (100) along the a^* axis (Fig. 1) and compared with the corresponding part of $ZnSiO_3(O)$ (Fig. 2) and $ZnMgSi_2O_6(O)$ (Fig. 3). One of the features of the $ZnSiO_3(M)$ structure is the coordination of oxygen atoms to and the position of Zn atoms in the M2 and M1 polyhedra. As shown in Fig. 1, Zn(2) in the M2 site is situated far from O(3) and close to O(1) and O(2). The bond lengths Zn(2)–O(1) and Zn(2)–O(2) (Table 6) are 1·933 and 2·031 Å, respectively. No bonding is observed between Zn(2) and O(3) which have interatomic distances greater than 3·0 Å. This results in an irregular tetrahedral coordination of O(1) and O(2) atoms around Zn(2). A similar tendency is shown by Zn(1) in the M1 octahedra, where Zn(1) is displaced far from the edge [O(1)–O(1)] shared with the M2 tetrahedra. However, Zn(1) has a rather regular octahedral coordination with four short bonds of 2·018 and 2·084 Å and two slightly long bonds of 2·333 Å.

Table 6. *Interatomic distances* (Å) *and angles* (°) *in* $ZnSiO_3(M)$

M1 site		M2 site	
Zn(1)—O(1A')	2·333 (3)	Zn(2)—O(1A)	2·031 (3)
–O(1A)	2·018 (3)	–O(1B)	2·031 (3)
–O(2C')	2·084 (3)	–O(2C')	1·933 (2)
Mean	2·145	–O(2D')	1·933 (2)
		Mean	1·982
O(1B')–O(1B)	3·089 (4)	O(1A) –O(1B)	3·003 (5)
–O(1A)	2·847 (3)	–O(2C')	3·012 (4)
–O(2D)	3·169 (4)	–O(2D')	2·807 (4)
–O(2C)	2·807 (4)	O(1B)—O(2C')	2·807 (4)
O(1B)—O(1A)	3·003 (5)	–O(2D')	3·012 (4)
–O(1A')	2·847 (4)	O(2C')–O(2D')	3·839 (4)
–O(2D)	3·185 (4)	–O(3C)	2·588 (4)
O(1A) –O(1A')	3·089 (4)	–O(3D')	3·169 (4)
–O(2C)	3·185 (4)	O(2D')–O(3C')	3·169 (4)
O(1A')–O(2D)	2·807 (4)	–O(3D)	2·588 (4)
–O(2C)	3·169 (4)	O(3C)–O(3D')	3·021 (4)
O(2C)–O(2D)	3·100 (4)	O(3D)–O(3D')	2·683 (4)
Mean	3·025		
SiO_4 tetrahedron			
Si——O(1)	1·617 (3)	O(1)——O(3′)	2·610 (4)
–O(2)	1·604 (3)	–O(2)	2·722 (4)
–O(3′)	1·627 (3)	–O(3)	2·609 (4)
–O(3)	1·625 (3)	O(2)——O(3′)	2·588 (4)
Mean	1·618	–O(3)	2·638 (4)
Si——O(3)–Si′	141·6 (2)	O(3)——O(3′)	2·683 (4)
O(3′)–O(3)–O(3″)	161·3 (1)	Mean	2·642

The mean bond length of 1·982 Å for Zn(2)–O is observed in the tetrahedral coordination of Zn in Zn_2SiO_4II (1·98 Å) (Marumo & Syono, 1971), hemimorphite (1·96 Å) (McDonald & Cruickshank, 1967) and other compounds. The effective ionic radii of Shannon & Prewitt (1967) give the bond length of 2·00 Å for the tetrahedral coordination and the tetrahedral covalent bond of Pauling (1960) gives 1·97 Å. The mean bond length of 2·145 Å of Zn(1)–O in the M1 octahedron is also frequently observed for octahedrally coordinated Zn. The octahedra of Zn(1) and tetrahedra of Zn(2) form rectangular slabs elongated along the c axis, and connected by SiO_3 chains.

The irregular coordination around Zn also strongly affects the shape of the SiO_3 chain. The average length of Si–O(nbr: non-bridging oxygen) is 1·611 Å, while that of Si–O(br: bridging oxygen) is 1·626 Å. The difference of 0·015 Å is much smaller than that for the case where divalent cations have six or eight coordination at the M2 site, *e. g.* 0·082 Å for diopside (Clark, Appleman & Papike, 1969), 0·084 Å for johannsenite (Freed & Peacor, 1967) *etc.*, and is almost same as for the case of monovalent cations, *e. g.* 0·012 Å for spodumene (Clark *et al.*, 1969) and 0·019 Å for jadeite

† A list of structure factors has been deposited with the British Library Lending Division as Supplementary Publication No. SUP 30796 (37 pp., 1 microfiche). Copies may be obtained through The Executive Secretary, International Union of Crystallography, 13 White Friars, Chester CH1 1NZ, England.

(Prewitt & Burnham, 1966) *etc.* This change in the Si–O bond distance in the chains is considered to take place by the displacement of Zn in the M2 site away from the SiO_3 chains, resulting in a weaker interaction between Zn and O(3).

Another feature of the SiO_3 chain in $ZnSiO_3(M)$ is the straightness of the chains indicated by the angle O(3′)–O(3)–O(3″) of 161·3°. This is the smallest value of the angle O(3′)–O(3)–O(3″) in the monoclinic pyroxenes in space group $C2/c$

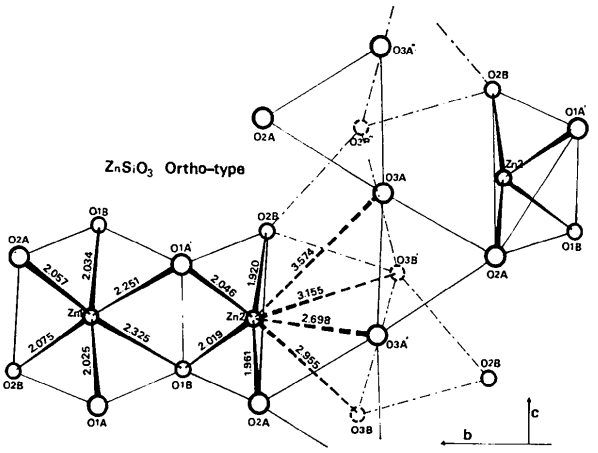

Fig. 2. Part of the structure of $ZnSiO_3$ (*O*) projected on (100) along the *a* axis. Zn(2) is still tetrahedrally coordinated, but some of the O(3) atoms approach Zn(2) to form an irregular octahedral arrangement.

(*b*) $ZnSiO_3(O)$

The structure of $ZnSiO_3(O)$ (Fig. 2) is not much different from that of enstatite (Morimoto & Koto, 1969). Some selected interatomic distances and angles are presented in Table 7.

Although the structure of $ZnSiO_3(O)$ is different from that of $ZnSiO_3(M)$ in that $ZnSiO_3(O)$ has two crystallographically different SiO_3 chains (*A* chain and *B* chain), a similar displacement of Zn atoms is observed in the M1 and M2 polyhedra. For the M1 site, Zn(1) is slightly displaced away from Zn(2) at the M2 site (Fig. 2), and is coordinated by six oxygen atoms octahedrally. There are four oxygen atoms with bond lengths of 2·025–2·075 Å and two oxygen atoms with the bond length 2·288 Å. In the M2 site, Zn(2) is also displaced away from O(3) and towards O(1) and O(2).

Table 7. *Interatomic distances* (Å) *and angles* (°) *in* $ZnSiO_3(O)$

M1 site		M2 site	
Zn(1)—O(1*A*′)	2·251 (6)	Zn(2)—O(1*A*)	2·046 (6)
–O(1*B*)	2·325 (6)	–O(1*B*)	2·019 (6)
–O(1*A*)	2·025 (6)	–O(2*A*)	1·961 (6)
–O(1*B*′)	2·304 (6)	–O(2*B*)	1·920 (6)
–O(2*A*)	2·057 (6)	–O(3*A*′)	2·688 (6)
–O(2*B*)	2·075 (6)	–O(3*B*)	2·955 (6)
Mean	2·128	Mean	2·265
O(1*A*)–O(1*A*′)	3·054 (8)	O(1*A*)–O(1*B*)	2·948 (8)
–O(1*B*)	2·835 (8)	–O(2*A*)	2·955 (8)
–O(2*A*)	3·152 (8)	–O(2*B*)	2·776 (8)
–O(2*B*)	2·776 (8)	O(1*B*)–O(2*A*)	2·811 (8)
O(1*A*′)–O(1*B*)	2·948 (8)	–O(2*B*)	3·018 (8)
–O(1*B*′)	2·835 (8)	O(2*A*)–O(2*B*)	3·864 (8)
–O(2*A*)	3·074 (8)	–O(3*A*′)	2·553 (9)
O(1*B*)–O(1*B*′)	3·094 (9)	–O(3*B*)	3·130 (8)
–O(2*B*)	3·215 (8)	O(2*B*)–O(3*B*′)	2·616 (8)
O(1*B*′)–O(2*A*)	2·811 (8)	O(3*A*′)–O(3*B*)	3·016 (8)
–O(2*B*)	3·155 (8)	–O(3*B*′)	2·929 (8)
O(2*A*)–O(2*B*)	3·052 (8)	O(3*B*)–O(3*B*′)	2·737 (8)
Mean	3·000		

SiO_4 tetrahedra

A chain		*B* chain	
Si(*A*)—O(1*A*)	1·618 (6)	Si(*B*)—O(1*B*)	1·622 (6)
–O(2*A*)	1·610 (6)	–O(2*B*)	1·611 (6)
–O(3*A*′)	1·637 (6)	–O(3*B*)	1·653 (6)
–O(3*A*)	1·620 (6)	–O(3*B*′)	1·631 (6)
Mean	1·621	Mean	1·629
O(1*A*)–O(3*A*′)	2·629 (8)	O(1*B*)–O(3*B*′)	2·612 (8)
–O(2*A*)	2·732 (8)	–O(2*B*)	2·735 (8)
–O(3*A*)	2·662 (8)	–O(3*B*)	2·616 (8)
O(2*A*)–O(3*A*′)	2·656 (9)	O(2*B*)–O(3*B*′)	2·642 (8)
–O(3*A*)	2·553 (9)	–O(3*B*)	2·616 (8)
O(3*A*)–O(3*A*′)	2·639 (9)	O(3*B*)–O(3*B*′)	2·737 (8)
Mean	2·645	Mean	2·660
Si′——O(3*A*)–Si	141·0 (4)	Si′——O(3*B*)–Si	136·7 (4)
O(3*A*′)–O(3*A*)–O(3*A*″)	178·3 (4)	O(3*B*′)–O(3*B*)–O(3*B*″)	149·2 (3)

In addition to the four oxygen atoms at a mean bond length of 1·987 Å, two O(3) atoms approach Zn(2) at distances of 2·698 and 2·955 Å, because of the deformation of the *A* and *B* chains. The coordination of Zn(2) is, therefore, rather similar to that in enstatite and orthoferrosilite with six coordination. In the *A* and *B* chains, O(3′)–O(3)–O(3″) angles are 178·3° and 149·2°, respectively, compared with 161·3° in $ZnSiO_3(M)$. The Si–O distances are 1·621 and 1·629 Å in the *A* and *B* chains, respectively, which are slightly longer than those in $ZnSiO_3(M)$. The differences between Si–O(br) and Si–O(nbr) are 0·014 and 0·026 Å in the *A* and *B* chains, respectively, both of which are still smaller compared with those in enstatite and orthoferrosilite, indicating the effect of displacement of Zn.

(*c*) $ZnMgSi_2O_6(O)$

A part of the structure of $ZnMgSi_2O_6(O)$ is shown in Fig. 3 in projection (as in Fig. 1). Some selected interatomic distances and angles are presented in Table 8. Zn atoms are partially ordered in the M1 and M2 sites with site occupancies of 36 and 64% respectively. The structural study of $Zn_{0.45}Mg_{1.55}Si_2O_6(O)$, carried out by Ghose, Okamura, Wan & Ohashi (1974), indicates the site occupancy of M1 (Zn 0·067, Mg 0·933) and M2 (Zn 0·383, Mg 0·617). More studies are necessary for an understanding of the site preference of Zn for the M1 and M2 sites.

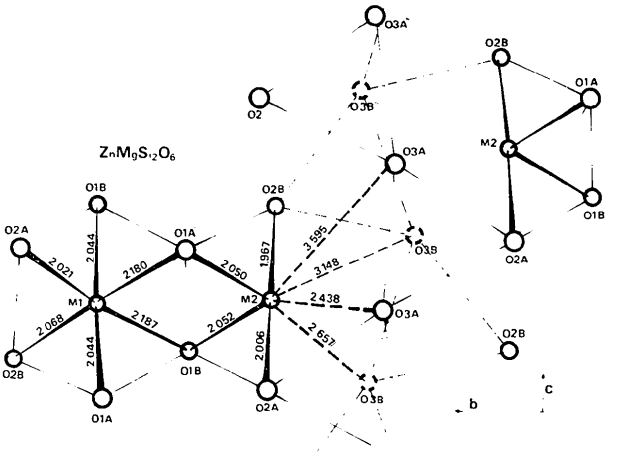

Fig. 3. Part of the structure of $ZnMgSi_2O_6(O)$ projected on (100) along the *a* axis. The tetrahedral arrangement around the M2 site is less remarkable.

Table 8. *Interatomic distances* (Å) *and angles* (°) *in* $ZnMgSi_2O_6(O)$

M1 site		M2 site	
M1——O(1*A*′)	2·180 (12)	M2——O(1*A*)	2·050 (11)
–O(1*B*)	2·187 (11)	–O(1*B*)	2·052 (11)
–O(1*A*)	2·044 (11)	–O(2*A*)	2·006 (10)
–O(1*B*′)	2·044 (11)	–O(2*B*)	1·967 (10)
–O(2*A*)	2·021 (11)	–O(3*A*′)	2·438 (11)
–O(2*B*)	2·068 (10)	–O(3*B*)	2·657 (10)
Mean	2·091	Mean	2·195
O(1*A*) –O(1*A*′)	3·037 (16)	O(1*A*) –O(1*B*)	2·835 (15)
–O(1*B*)	2·826 (15)	–O(2*A*)	2·885 (15)
–O(2*A*)	3·048 (15)	–O(2*B*)	2·785 (14)
–O(2*B*)	2·785 (14)	O(1*B*)–O(2*A*)	2·802 (14)
O(1*A*′)–O(1*B*)	2·835 (15)	–O(2*B*)	3·012 (14)
–O(1*B*′)	2·826 (15)	O(1*B*)–O(3*B*)	3·317 (15)
–O(2*A*)	2·982 (16)	O(2*A*) –O(2*B*)	3·969 (14)
O(1*B*)–O(1*B*′)	3·030 (15)	–O(3*A*′)	2·536 (15)
–O(2*B*)	3·166 (15)	–O(3*B*)	3·111 (14)
O(1*B*′)–O(2*A*)	2·802 (14)	O(2*B*)–O(3*A*)	3·310 (14)
–O(2*B*)	3·120 (14)	–O(3*B*′)	2·568 (14)
O(2*A*) –O(2*B*)	2·957 (14)	O(3*A*′)–O(3*B*)	2·928 (14)
Mean	2·951		

SiO_4 tetrahedra

A chain		*B* chain	
Si——O(1*A*)	1·612 (11)	Si——O(1*B*)	1·642 (11)
–O(2*A*)	1·610 (12)	–O(2*B*)	1·569 (10)
–O(3*A*)	1·651 (12)	–O(3*B*)	1·679 (11)
–O(3*A*′)	1·626 (12)	–O(3*B*′)	1·638 (11)
Mean	1·625	Mean	1·633
O(1*A*) –O(3*A*′)	2·610 (15)	O(1*B*)–O(3*B*′)	2·641 (14)
–O(2*A*)	2·725 (15)	–O(2*B*)	2·748 (14)
–O(3*A*)	2·709 (15)	–O(3*B*)	2·625 (14)
O(2*A*) –O(3*A*′)	2·696 (15)	O(2*B*)–O(3*B*′)	2·656 (14)
–O(3*A*)	2·536 (15)	–O(3*B*)	2·568 (14)
O(3*A*) –O(3*A*′)	2·621 (16)	O(3*B*)–O(3*B*′)	2·741 (15)
Mean	2·663	Mean	2·663
Si——O(3*A*) –Si′	137·7 (7)	Si——O(3*B*)–Si′	131·5 (7)
O(3*A*′)–O(3*A*) –O(3*A*″)	166·9 (6)	O(3*B*′)–O(3*B*)–O(3*B*″)	143·6 (5)

The structure of $ZnMgSi_2(O)_6$ is intermediate between that of enstatite and $ZnSiO_3(O)$. Zn(1) atoms are near the centres of rather regular octahedra of oxygen atoms as in enstatite (Morimoto & Koto, 1969). However, Zn(2) atoms are located in deformed octahedra with four oxygen atoms at mean distances of 2·019 Å and (two) of 2·548 Å. The shapes of the *A* and *B* chains are also intermediate between those of $ZnSiO_3(O)$ and enstatite, and their O(3′)–O(3)–O(3″) angles are 166·9° and 143·5°, respectively. The difference between Si–O(br) and Si–O(nbr) becomes appreciable with values of 0·027 Å for the *A* chain and 0·053 Å for the *B* chain, because of the approach of M2 to O(3).

(*d*) *The structural relations between* $ZnSiO_3(M)$ *and* $ZnSiO_3(O)$

The structures of $ZnSiO_3(M)$ and $ZnSiO_3(O)$ are compared in Fig. 4. In the $ZnSiO_3$ polymorphs, one of the remarkable differences between the structures is the position of O(3) which results in the different coordinations of Zn(2). When we consider, however, only the octahedral arrangement of Zn(1) and tetrahedral arrangement of Zn(2) the structural units consisting of the Zn polyhedra are practically identical in both structures. They are superposed in Fig. 4 to illustrate the difference in the arrangement of the SiO_3 chains in both structures. $ZnSiO_3(M)$ in $C2/c$ has only one type of SiO_3 chain, while $ZnSiO_3(O)$ has two types. To obtain the *A* and *B* chains of $ZnSiO_3(O)$ starting from the chains of $ZnSiO_3(M)$, we have to consider the rotation of the SiO_4 tetrahedra (Thompson, 1970; Papike, Prewitt, Sueno & Cameron, 1973). However, the axes of rotation in $ZnSiO_3(O)$ are not the lines connecting Si and O(1) of the tetrahedra, but those through the shared corners, O(2), of the tetrahedra and the Zn(1) octahedra. In spite of the difference in straightness of the chains in both structures, their *c* lengths remain almost constant through the change in the O(3)–O(3′) distances and O(3′)–O(3)–O(3″) angles. The O(3)–O(3′) distances and O(3′)–O(3)–O(3″) angles are, 2·683 Å and 161·3°, 2·659 Å and 178·3°, and 2·737 Å and 149·2°, for the chain in $ZnSiO_3(M)$, and the *A* and *B* chains in $ZnSiO_3(O)$ respectively.

It is well known that the orthorhombic pyroxenes are considered to be repeated unit-cell twins of monoclinic pyroxenes in $P2_1/c$; that is, the orthorhombic unit cell is composed of two monoclinic unit cells of $P2_1/c$ twinned by a *b*-glide plane parallel to (100) (Ito, 1950; Morimoto & Koto, 1969; Smith, 1969). In the case of $ZnSiO_3$ polymorphs, the tendency of Zn atoms to maintain tetrahedral coordination is stronger in $ZnSiO_3(M)$ than in $ZnSiO_3(O)$, and it seems difficult for $ZnSiO_3$ to exist as a monoclinic pyroxene in $P2_1/c$ where the M1 and M2 sites are octahedrally coordinated. The unit-cell twin relation (Ito, 1950) observed

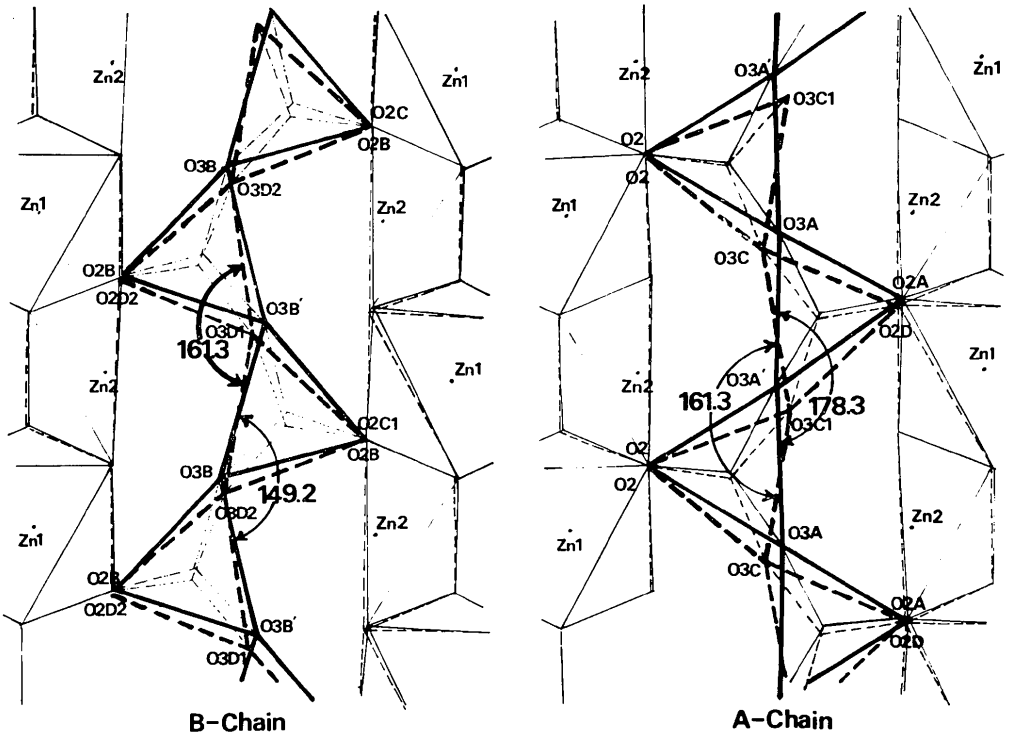

Fig. 4. Comparison of the structures of $ZnSiO_3(M)$ and $ZnSiO_3(O)$. The bands consisting of the Zn polyhedra are almost identical in both polymorphs, and are superposed. The SiO_3 chains of $ZnSiO_3(M)$ are shown by broken lines and the *A* and *B* chains of $ZnSiO_3(O)$ by full lines.

between the orthorhombic and monoclinic polymorphs of $MgSiO_3$ (Morimoto & Koto, 1969) and $FeSiO_3$ (Burnham, 1967) is not applicable to $ZnSiO_3$. Thus $ZnSiO_3$ represents a special case of a pyroxene structure in which a monoclinic type in $C2/c$ has a polymorph of orthorhombic type in *Pbca*. This uniqueness of $ZnSiO_3$ may explain why the orthorhombic polymorph with an octahedral arrangement of Zn(2) cannot be stable under any condition as shown by Syono, Akimoto & Matsui (1971).

Of special interest as regards high-pressure experiments is that $ZnSiO_3(O)$ is denser than $ZnSiO_3(M)$ by more than 1%. This is in clear contrast to $MgSiO_3$, $FeSiO_3$ and $CoSiO_3$ pyroxenes for which the density of the monoclinic phases is almost same as or greater than that of their orthorhombic phases. This uniqueness in density for the polymorphs of $ZnSiO_3$ pyroxenes is explained by the structure of $ZnSiO_3(M)$ in $C2/c$ in which the M2 polyhedron is more open than that in $ZnSiO_3(O)$.

(e) *Large β angle of* $ZnSiO_3(M)$

In order to discover why $ZnSiO_3(M)$ has an exceptionally large β angle (111·42°) in the monoclinic pyroxenes in $C2/c$, the structure of $ZnSiO_3(M)$ is compared with that of johannsenite ($CaMnSi_2O_6$) which has the smallest β angle. The cell dimensions of johannsenite are $a=9{\cdot}915$, $b=9{\cdot}107$, $c=5{\cdot}280$ Å and $\beta=105{\cdot}2°$, and the structure is very close to that of diopside (Freed & Peacor, 1967). Because the c lengths are nearly equal in the structures of $ZnSiO_3(M)$ and johannsenite, both structures are projected on (010) with the metal atoms in the central part of the unit cells at the same positions as in Fig. 5.

There are two ways in which the β angle can be made larger in the structure of the monoclinic pyroxenes: by bringing the neighbouring SiO_3 chains closer and by displacing the SiO_3 chains along the c axis. A combination of these two displacements of the SiO_3 chains is also possible.

The most characteristic difference between the two structures is in the positions of the SiO_3 chains relative to the metal sites. The former are clearly shown by the positions of the Si atoms in both structures.

The tetrahedral coordination around Zn(2) gives rise to short Zn(2)–O(1) and Zn(2)–O(2) distances. Because O(3) atoms are coordinated not by Zn(2) atoms but only by Si atoms, as described above, the relative

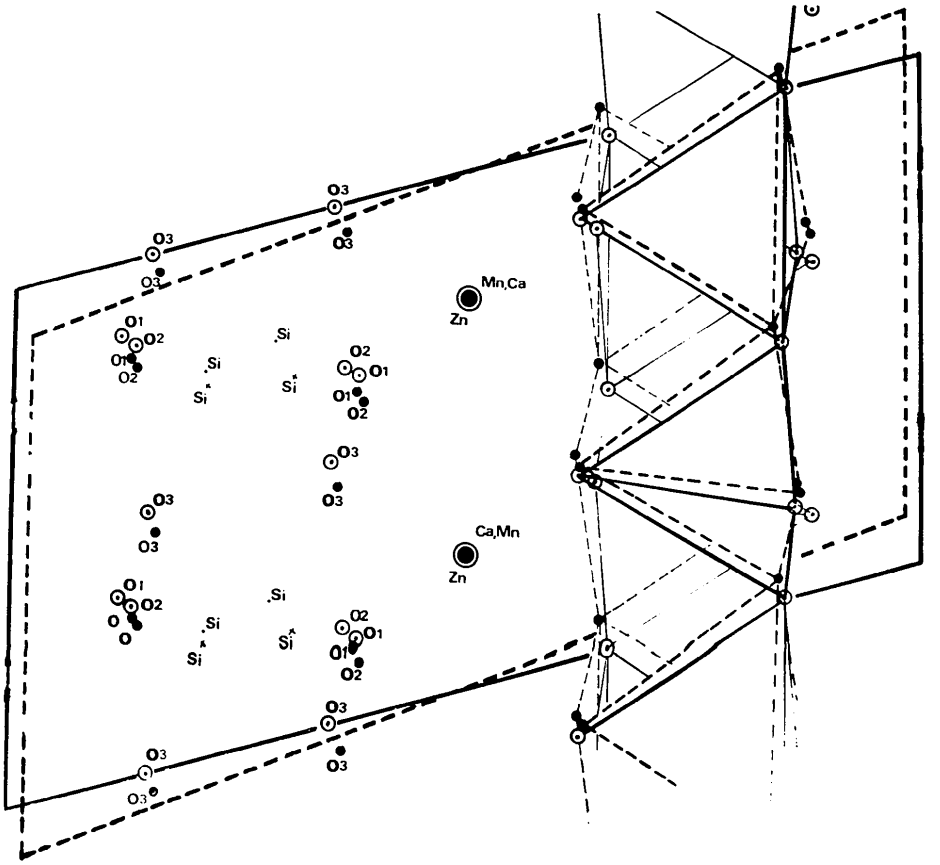

Fig. 5. Comparison between the structures of $ZnSiO_3(M)$ and johannsenite($CaMnSi_2O_6$). Both structures are projected on (010) with the metal atoms in the central part of each unit cell at the same position, in order to demonstrate the difference in the β angle in both structures. The SiO_3 chains of $ZnSiO_3(M)$ (shown by full lines) are compared with those of johannsenite (shown by broken lines) on the right of the diagram. Si atoms are shown by dots and crosses for $ZnSiO_3(M)$ and johannsenite, respectively, on the left.

position of the SiO_3 chains with respect to Zn atoms is mainly determined by the Zn(2)–O(1) and Zn(2)–O(2) distances. An apparent relative displacement of the SiO_3 chains along the c axis is clear in the structure of $ZnSiO_3(M)$ so that the β angle increases in comparison with the structure of johannsenite.

We wish to thank Drs K. Koto, H. Horiuchi and M. Tokonami, of the Institute of Scientific and Industrial Research, Osaka University, for their help in intensity measurements and their interest during the course of this study. Thanks are also due to Miss M. Hirano for typing the manuscript. Part of the cost of this work was defrayed by a research grant from the Japanese Ministry of Education.

References

BURNHAM, C. W. (1967). *Carnegie Inst. Wash. Year Book.* **65**, 285–290.
BURNHAM, C. W., CLARK, J. R., PAPIKE, J. J. & PREWITT, C. T. (1967). *Z. Kristallogr.* **125**, 109–119.
BUSING, W. R., MARTIN, K. O. & LEVY, H. A. (1962). *ORFLS.* Oak Ridge National Laboratory Report ORNL-TM-305.
CHRISTENSEN, A. N. & HAZELL, R. G. (1967). *Acta Chem. Scand.* **21**, 1425–1429.
CLARK, J. R., APPLEMAN, D. E. & PAPIKE, J. J. (1969). *Miner. Soc. Amer. Spec. Pap.* **2**, 31–50.
DEER, W. A., HOWIE, R. A. & ZUSSMAN, J. (1963). *Rock-Forming Minerals*, Vol. 2.
FREED, R. L. & PEACOR, D. R. (1967). *Amer. Min.* **52**, 709–720.
GHOSE, S., OKAMURA, F. P. WAN, C. & OHASHI, H. (1974). *Trans. Amer. Geophys. Union*, **55**, No. **4**, 467.
International Tables for X-ray Crystallography (1962). Vol. III, pp. 201–227. Birmingham: Kynoch Press.
ITO, T. (1950). *X-ray Studies of Polymorphism.* Tokyo: Maruzen.
LOUISNATHAN, S. J. (1969). *Z. Kristallogr.* **130**, 427–437.
MCDONALD, W. S. & CRUICKSHANK, D. W. J. (1967). *Z. Kristallogr.* **124**, 180–191.
MARUMO, F. & SYONO, Y. (1971). *Acta Cryst.* B**27**, 1868–1870.
MORIMOTO, N. & KOTO, K. (1969). *Z. Kristallogr.* **129**, 65–83.
PAPIKE, J. J., PREWITT, C. T., SUENO, S. & CAMERON, M. (1973). *Z. Kristallogr.* **138**, 254–273.
PAULING, L. (1960). *The Nature of the Chemical Bond.* Ithaca: Cornell Univ. Press.
PREWITT, C. T. & BURNHAM, C. W. (1966). *Amer. Min.* **51**, 956–975.
RENTZEPERIS, P. J. (1963). *Z. Kristallogr.* **119**, 117–138.
SAKURAI, T. (1967). Editor *Universal Crystallographic Computation Program System.* Tokyo: Crystallographic Society of Japan.
SHANNON, R. D. & PREWITT, C. T. (1969). *Acta Cryst.* B**25**, 925–946.
SMITH, J. V. (1969). *Miner. Soc. Amer. Spec. Pap.* **2**, 3–29.
SYONO, Y., AKIMOTO, S. & MATSUI, Y. (1971). *J. Solid State Chem.* **3**, 369–380.
TOKONAMI, M. (1965). *Acta Cryst.* **19**, 486.
THOMPSON, J. B. JR (1970). *Amer. Min.* **55**, 292.
WARREN, B. E. & BRAGG, W. L. (1928). *Z. Kristallogr.* **69**, 168–193.

Acta Cryst. (1975). B**31**, 1049

The Structure of the Cyclopentane Ring. 1-Phenylcyclopentanecarboxylic Acid

BY T. N. MARGULIS

Department of Chemistry, University of Massachusetts at Boston, Boston, Massachusetts 02125, *U.S.A.*

(*Received* 16 *August* 1974; *accepted* 27 *November* 1974)

The structure of 1-phenylcyclopentanecarboxylic acid, $C_{12}H_{14}O_2$, has been determined by analysis of 824 diffractometer-measured X-ray reflections and refined by least-squares calculations to an R of 0·066. The crystals are monoclinic, space group $P2_1/c$, $Z=4$, $a=6{\cdot}009$, $b=6{\cdot}781$, $c=24{\cdot}976$ Å, $\beta=92{\cdot}08°$. The cyclopentane ring is rigid with a conformation intermediate between the C_2 and C_s forms.

Introduction

The saturated five-carbon cyclopentane ring may exist in two symmetric, non-planar conformations. These are the envelope form with C_s symmetry (four carbon atoms in a plane and one out of plane) and the half-chair or twisted form with C_2 symmetry. These two forms are of about the same energy and lie about 5 kcal mole^{-1} below the planar structure with D_{5h} symmetry (Carreira, Jiang, Person & Willis, 1972). The C_2 form has been observed in *trans*-1,2-cyclopentanedicarboxylic acid (Benedetti, Corradini & Pedone, 1972) while the C_s form has been observed in several bicyclic systems (Chiang & Bauer, 1968). In addition to these two symmetric conformations, an infinite number of asymmetric conformations exists. These have about the same energy as the symmetric forms, so that the cyclopentane molecule rapidly converts from one to another. This process, called pseudorotation, has been demonstrated in the gas phase by electron diffraction (Adams, Geise & Bartell, 1970) and was used by Kilpatrick, Pitzer & Spitzer (1947) to explain the high-